Colloids and Surfaces A: Physicochem. Eng. Aspects 504 (2016) 228–233

Contents lists available at ScienceDirect

Colloids and Surfaces A: Physicochemical and Engineering Aspects

journal homepage: www.elsevier.com/locate/colsurfa

Synthesis method for crystalline hollow titania micron-cubes

Sonja I.R. Castillo[a,*], Nynke A. Krans[a], C.E. (Lisette) Pompe[b], J.H. (Arjan) den Otter[b], Dominique M.E. Thies-Weesie[a], Albert P. Philipse[a]

[a] Van 't Hoff Laboratory for Physical and Colloid Chemistry, Debye Institute for NanoMaterials Science, Utrecht University, Padualaan 8, 3584 CH Utrecht, The Netherlands
[b] Inorganic Chemistry and Catalysis, Debye Institute for NanoMaterials Science, Utrecht University, Universiteitsweg 99, 3584 CG Utrecht, The Netherlands

HIGHLIGHTS

- A straightforward synthesis method for cubic titania colloids is presented.
- The synthesis method only requires conventional chemicals and ambient conditions.
- Hollow and core–shell hematite@titania colloids are prepared.
- The cubic shape allows for the formation of dense colloidal arrays.

GRAPHICAL ABSTRACT

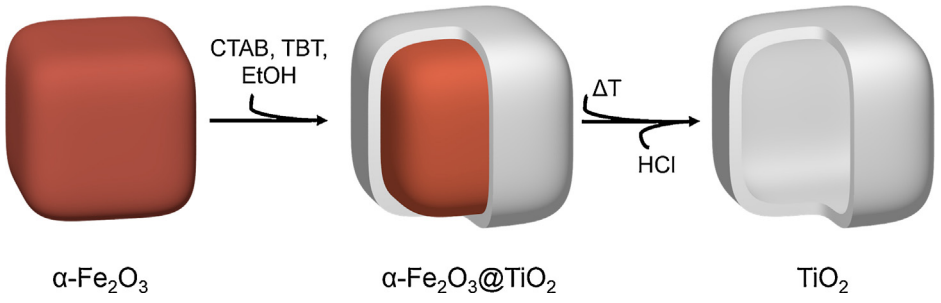

ARTICLE INFO

Article history:
Received 30 January 2016
Received in revised form 12 May 2016
Accepted 24 May 2016
Available online 27 May 2016

Keywords:
Anatase titania
Rutile titania
Cubic colloids
Cubes
Core–shell

ABSTRACT

We report the synthesis of novel micron-sized titania cubes comprising a hematite core and a titania shell. Single core particles are entirely coated with a homogeneous titania shell of tunable thickness. Our convenient and straightforward synthesis method is mediated by the surfactant cetyltrimethylammonium bromide (CTAB) and proceeds under ambient conditions. Subsequent calcination transforms the amorphous titania shell to anatase/rutile titania; dissolution of the hematite core eventually results in hollow porous titania cubes. The resulting core–shell and hollow titania cubes display the tendency to align face-to-face, indicating their potential for utilization in close-packed arrays.

1. Introduction

Titania particles are widely applied, e.g., as pigments [1,2], photocatalysts for degradation of organic compounds and for water-splitting [1,3–5], and components in photovoltaic devices [1,6–8]. Moreover, the mechanical and chemical robustness of titania contribute to its extensive use in ceramics, such as separation membranes [9,10]. Another emerging application of titania colloids lies in the field of photonic materials [11,12]. For especially the latter two applications, dense packings of colloids are of interest. Such particle packings are generally composed of spherical particles, resulting in a maximum volume fraction of circa 0.74 [13,14]. An increased volume fraction, on the other hand, can be obtained with more cube-shaped particles, up to 1 for perfect cubes [13,14]. Recently, the formation of dense arrays using colloidal cubes composed of silica and hematite has been demonstrated [15–18]. Due to the slightly rounded corners of the employed particles, the

* Corresponding author.

http://dx.doi.org/10.1016/j.colsurfa.2016.05.079
0927-7757/

maximum volume fraction that could be achieved was circa 0.87 [13,14]. Although not a perfectly dense packing, the achieved volume fraction was substantially higher than for spheres. In a similar way, it would be relevant to have such dense assemblies composed of titania building blocks as to combine the advantages of dense particle packings and the material properties of titania. As a first step towards this aim, we present here a convenient synthesis method for colloidal titania cubes.

Many of the listed applications actually only require titania at the surface of the particles, such that core–shell particles with a titania shell suffice. Unfortunately, the synthesis of titania coated colloids is notoriously challenging due to fast hydrolysis and condensation reactions of titania alkoxide precursors [19,20]. Therefore, numerous procedures employ titanium complexes as precursors [21,22], special stabilizers [23] or solvent mixtures [20,24] which retard reaction rates, but, unfortunately, at the same time complicate the synthesis. As an alternative to these procedures, we report a straightforward and reproducible synthesis method for titania shells grown directly onto micron-sized, cubic hematite (α-Fe_2O_3) cores. Titania growth occurs here at ambient conditions and with the use of the conventional titania precursor titanium(IV) butoxide (TBT) and as mediator, the surfactant cetyltrimethylammonium bromide (CTAB). Our procedure results in core–shell hematite@titania cubic colloids, which can subsequently be transformed to stable anatase/rutile titania cubes and which can even be made hollow by dissolution of the hematite cores. Notably, our method results in the formation of titania shells around single particles and aggregation is generally avoided. Eventually, the titania cubes could serve as building blocks of dense particle assemblies.

2. Materials and methods

2.1. Particle synthesis

2.1.1. Hematite cubes

Monodisperse cubic hematite particles were prepared following an adapted sol–gel method of Sugimoto et al. [17,25]. Typically, a mixture of aqueous solutions of iron(III) chloride (2.0 M, iron(III) chloride hexahydrate, p.a., Sigma–Aldrich) and sodium hydroxide (5.4 M, p.a., Emsure) was aged at 100 °C for eight days. The resulting sol was then washed by centrifugation and redispersion in Millipore water until pH ~7 was reached. Bigger cubes can be obtained by using a larger excess of iron(III) ions.

2.1.2. Core–shell hematite@titania cubes

The synthesis of titania coated hematite cubes is mediated by the surfactant cetyltrimethylammonium bromide (CTAB, 99%, Sigma–Aldrich) and typically proceeds as follows. Firstly, a mixture of 1.7 g (dry weight) hematite cubes and 420 mL aqueous CTAB solution (1.7 mM) was sonicated for 1 h. Secondly, an ethanolic titania precursor solution was made in a glovebox by mixing 4.5 g titanium(IV) butoxide (TBT, reagent grade 97%, Sigma–Aldrich) with 67.5 mL absolute ethanol (Merck). Subsequently, the following was added at ambient conditions to a 1 L round bottom flask while sonicating at 20 °C: 360 mL absolute ethanol, 15 mL Millipore water and the cubes/CTAB mixture. Next, 67.5 mL of the TBT solution was quickly added with a dropping funnel. The reaction mixture was then sonicated for an additional 8 min after which it was washed five times by centrifugation and redispersion in ethanol. To ensure all titania aggregates resulting from secondary nucleation were removed, a decreasing centrifugation speed was applied in each consecutive washing step: 500 g, 450 g, 350 g, 150 g and 50 g. The cubes were eventually redispersed in 420 mL absolute ethanol. The resulting cubes were then coated again following the method described above, but without the addition of CTAB. The final sediment was redispersed in 210 mL absolute ethanol.

2.1.3. Calcined and hollow titania cubes

For the calcination process, dried cubes were first heated at 60 °C for 1 h (heating rate 80 °C/h from 20 °C to 60 °C) and then at 450 °C for 3 h (heated from 60 °C to 450 °C in 6.5 h). The thermal treatments were performed in air and with a Nabertherm N15/65 HA oven. The dry calcined particles were redispersed in 30 mL absolute ethanol.

Hollow titania cubes were produced by treating calcined core–shell cubes with hydrochloric acid (6 M, Merck) to dissolve the hematite core. Complete dissolution was marked by a color change of the dispersion from red to yellow, caused by the dissolution of hematite to iron(III) ions and chloride ions. Complete dissolution was typically achieved within a few hours. The dispersion was then washed with Millipore water until pH ~7 was reached. The acid treatment to obtain hollow titania cubes should only be performed on calcined core–shell hematite@titania cubes which have a crystalline titania shell; amorphous titania cannot withstand the acid treatment and dissolves on a time scale similar to the hematite core.

2.2. Characterization

The cross-sectional appearance, average particle size and thickness of the produced titania shells were analyzed with Transmission Electron Microscopy (TEM), see Fig. 2B. The average size was determined from the edge length of at least 100 particles. The coating thickness was calculated by subtracting the average size of the core particles from the average size of the core–shell cubes. TEM samples were prepared by drop-casting diluted dispersion onto a polymer coated, carbon sputtered copper grid and were dried under a heating lamp. The employed Transmission Electron Microscopes were a Philips Tecnai 12 (120 kV) and Tecnai 10 (100 kV). The morphology and surface of the cubes were investigated with high resolution Scanning Electron Microscopy (SEM). SEM samples were made by sticking a TEM sample on a stub using a conductive carbon sticker. The entire SEM sample was then coated with a layer of platinum of typically 6 nm prior to analysis with a FEI XL30 FEG operated at 5–15 kV. With the employed SEM, elemental analysis with energy dispersive X-ray spectroscopy (EDX) of the particles was also performed.

Infrared spectra were recorded with a Perkin Elmer Frontier FT-MIR Spectrometer using KBr pellets as medium.

Wide-angle powder X-ray diffraction (XRD) measurements were performed at room temperature on a Bruker-AXS D2 Phaser Diffractometer using Co Kα radiation (λ = 1.78897 Å) and operated at 30 kV and 10 mA. The employed step size was 0.0991° in the angle range of $15° \leq 2\theta \leq 80°$.

Nitrogen physisorption measurements were performed on a Micromeritics TriStar 3000. The cubes were dried under a nitrogen gas flow prior to measurement, first overnight in a sample concentrator at 60 °C and then further overnight at 180 °C with a Micromeritics Smartprep. The specific surface area was derived by fitting the Brunauer–Emmett–Teller (BET)-isotherm in the linear relative pressure range p/p_0 = 0.06–0.25 of the measured adsorption isotherm. Barrett–Joyner–Halenda (BJH) analysis was performed to determine the pore size distributions [26].

3. Results and discussion

The synthesis of hollow cubic anatase/rutile titania particles comprises four stages. The first stage is the synthesis of hematite (α-Fe_2O_3) cubes, which act as the shape template. Following [17,25], we synthesize monodisperse hematite cubes, the edge length of which can be varied between 500 nm and 1500 nm. In this study, we employ hematite particles with a highly cubic shape and an

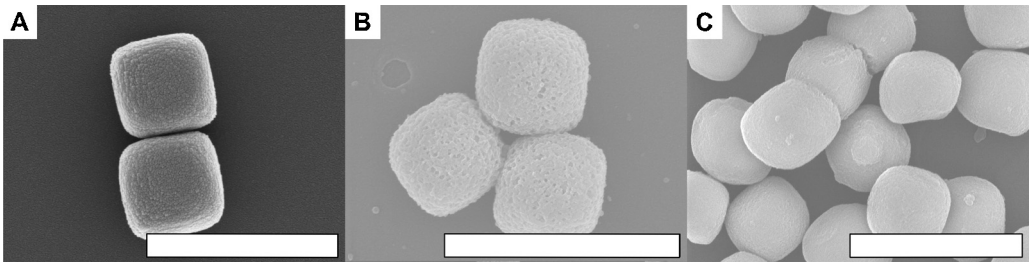

Fig. 1. Typical SEM images of cubes resulting after multiple titania coating steps. The scale bars represent 2 μm. The formation of a titania shell is evident from the change in the surface morphology compared to the bare hematite cubes in (A). (B) The first coating step yields titania cubes that retain their cubic shape and remain single particles. (C) After the second coating step, mostly single cubes and an occasional doublet or triplet are observed. The final titania coating thickness is ~60 nm.

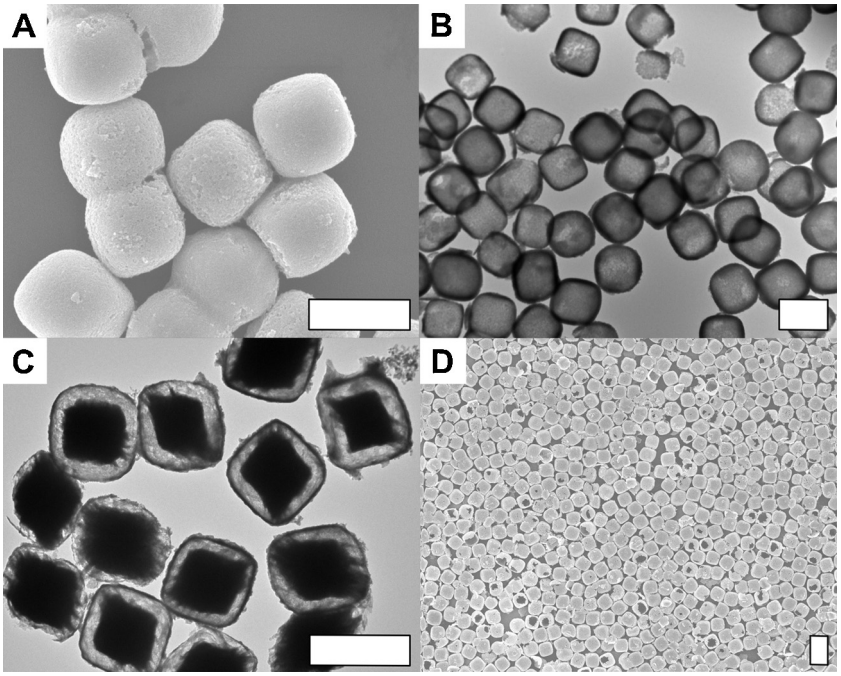

Fig. 2. Representative electron microscopy images of titania cubes after calcination. All scale bars represent 1 μm. (A) The titania shells remain intact after calcination. On a rare occasion, cracked cubes are present, resulting from previously attached cubes. (B) TEM image of calcined hollow titania particles that still display the cubic shape, indicating that the formed titania shell entirely and uniformly covers the cubes. (C) Rattle-like titania cubes with a hematite core are obtained by partially dissolving the hematite core. (D) SEM image of a monolayer of titania cubes produced by convective assembly. The cubes have the tendency to align face-to-face.

average edge length of 798 nm (Fig. 1A), but other cube sizes are similarly suitable. Secondly, the hematite cubes are coated with an amorphous titania shell to create core–shell hematite@titania cubes. This coating synthesis proceeds in ethanol in the presence of the surfactant CTAB, water, and the titania precursor TBT. A single coating step takes only 8 min, followed by washing steps. Multiple coating steps are performed to increase the thickness of the titania shell. In the third stage, crystalline titania is obtained by heating the core–shell cubes at 450 °C. Finally, dissolution of the hematite core with hydrochloric acid yields hollow cubes composed of crystalline titania.

Scanning electron microscopy (SEM) images of the cubes resulting after the first two stages are displayed in Fig. 1. The initial hematite cubes have a rough surface, which changes after the first coating step, confirming successful formation of a titania shell. After two coating steps, the core–shell hematite@titania particles still have a cubic shape and smooth titania shell. The majority of the particles are single cubes; apart from an occasional doublet or triplet, no clusters are observed after the second coating step. Size measurements corroborate the formation of a titania shell: the cubes grow from 798 nm (6% polydispersity) to 849 nm (5% polydispersity) after the first coating step and eventually to 921 nm (6% polydispersity), resulting in a final titania shell thickness of approximately 60 nm. Increasing the shell thickness should proceed by multiple coating steps; doubling the amount of titania precursor used per coating step merely yields more secondary titania nucleation.

In the third stage, crystalline titania is obtained by heating the core–shell cubes at 450 °C. Fig. 2A beautifully shows that the titania shells remain intact after calcination. Remarkably stable hollow titania cubes are finally obtained by acid treatment (Fig. 2B). Stopping the acid treatment before complete dissolution of the hematite core leads to rattle-like cubes, in which a small hematite core rattles around, i.e. moves freely, inside the titania cube (Fig. 2C). The advantage of the hematite core is its catalytic activity [17]. Reducing the size contributes to a large catalytically active area [17], while the titania shell maintains the cubic shape valuable for dense particle packings.

Energy dispersive X-ray spectroscopy and infrared spectroscopy confirm that the coatings are composed of titania. The wide-angle powder X-ray diffraction (XRD) patterns in Fig. 3A show that the titania in the core–shell hematite@titania cubes is initially amorphous, since only the hematite peaks are visible. The amorphous titania is transformed to crystalline titania after calcination,

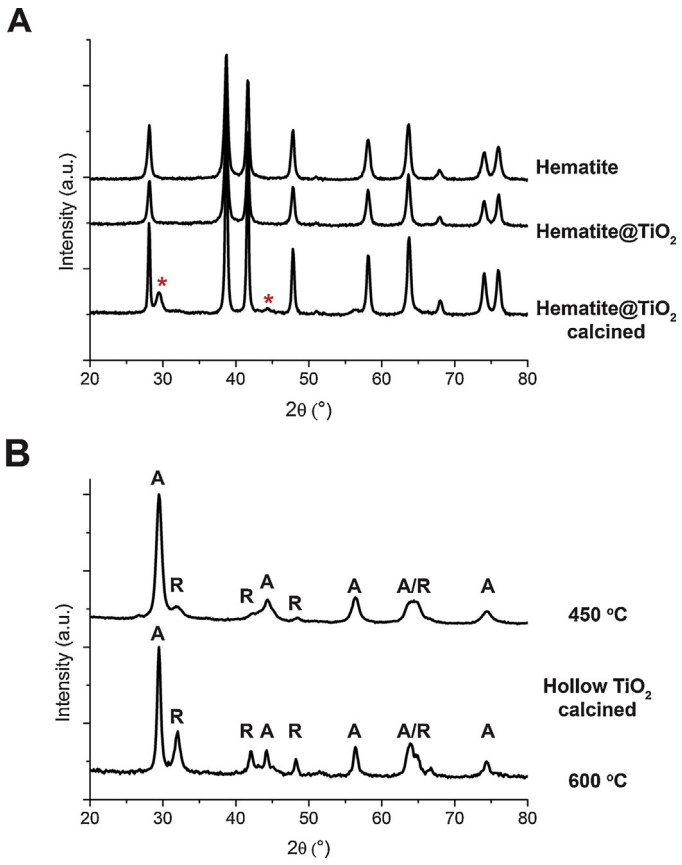

Fig. 3. Powder XRD data of titania cubes. (A) XRD patterns show that the titania is amorphous before calcination. Peaks of crystalline titania appear after calcination, indicated by the red asterisks. (B) XRD patterns of hollow titania cubes, calcined at 450 °C or 600 °C. Both the crystalline phases anatase (A) and rutile (R) are present.

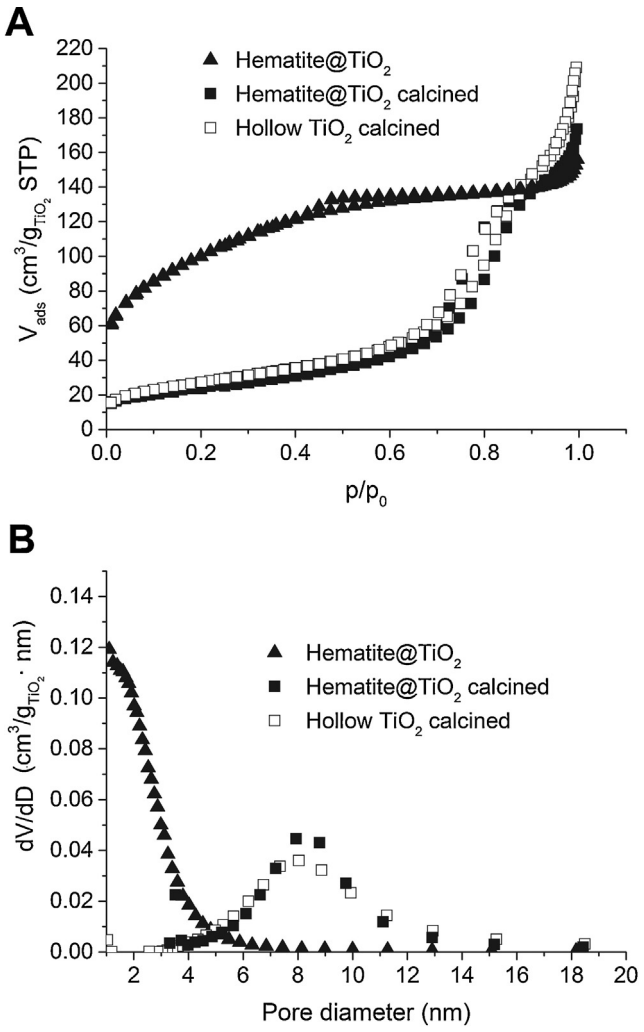

Fig. 4. Nitrogen physisorption data of titania cubes. (A) Physisorption isotherms of titania cubes, normalized to the amount of titania present. Densification occurs after calcination. (B) Pore size distributions of titania cubes, normalized to the amount of titania present. The mesoporous structure of the crystalline titania shells remains unaltered after acid treatment.

indicated by the appearance of additional peaks (marked by asterisks in Fig. 3A). These peaks are better visible in the XRD pattern of hollow calcined titania cubes displayed in Fig. 3B and reveal that both anatase (A) and rutile (R) are present. The mass percentage of rutile is ~28% after calcination at 450 °C and as expected, increases to ~40% when the calcination temperature is raised to 600 °C, as calculated via the method of Spurr et al. [27,28].

Phase transformation by calcination induces shrinkage of the titania coating, by approximately 50% from ~60 nm to ~30 nm in thickness [12,23,29,30]. Although shrinkage is often accompanied by deformation of the titania structure [30], our titania shells remain uniformly distributed over the hematite core after calcination. Hollow titania cubes with an intact and uniform shell verify this result (Fig. 2B). We attribute this significant result to the concomitant thermal removal of CTAB molecules during calcination, which creates space for the titania shell to shrink uniformly. In the incidental case of two adhered cubes, cleavage of the two cubes during calcination produces a crack, for instance visible in Fig. 2A. As a disadvantage, these cracks lead to holes in the titania shells of the detached cubes since the surface between them is obviously not coated with titania (Fig. S1). Fortunately, since the majority of the cubes are single particles, only a small fraction of titania cubes contain such defects.

The physisorption isotherms in Fig. 4A show that calcination and consequently, shrinkage of titania result in its densification. Correspondingly, the Brunauer–Emmett–Teller (BET)-surface area of titania shells drastically reduces from 274 m^2/g_{TiO_2} to 99 m^2/g_{TiO_2} after calcination. The isotherms and BET-surface areas have been normalized to the amount of titania in each sample using the appropriate titania mass percentage; the calculations are detailed in the Supplementary Information. Moreover, Fig. 4B shows that the pores in the titania shells are mesoporous. These mesopores originate from the titania shell, since the hematite core particles do not contain pores in the relevant pore size range (Fig. S2). The mesopores are considered to be a result of the thermal removal of the CTAB molecules, seeing as such pore templating by surfactants is well-established and nonporous titania is known to be formed when no surfactants are used [31–36]. Advantageously, dissolution of the hematite core does not affect the BET-surface area nor the pore structure of the crystalline titania. The presence of mesopores in the titania shell opens up additional possible applications of the titania cubes. For instance, nanoreactors for catalysis reactions benefit from an enhanced accessibility of the core resulting from mesopores [37,38].

Other studies using CTAB to mediate the formation of titania structures mainly involve the synthesis of solid titania spheres or titania thin films [34,35,39]. To the best of our knowledge, the preparation of titania coated colloids in the presence of CTAB has only been reported for silver nanoparticles that require stabilization with CTAB [40]. Our cubes, however, do not require steric stabilization and CTAB is added intentionally to induce the formation of titania coatings on seed particles. The reason why core–shell hematite@titania particles are successfully obtained in the

presence of CTAB is very likely twofold. On the one hand, species that carry quaternary ammonium groups are reported to have a positive effect on the hydrolysis and condensation of titania precursors, e.g., CTAB [34,35,40], ammonia [20,9], and glycine [32]. On the other hand, CTAB is an amphiphilic molecule that readily adsorbs onto the hematite surface. Therefore, the positively charged quaternary ammonium ions at the hematite cube surface create an attractive surface for the deposition of titania primary particles or oligomers and at the same time, promote titania polymerization. We will leave it at this qualitative assessment: the detailed formation mechanism using CTAB falls outside the scope of this study.

The beneficial ability of the titania cubes to form assemblies with high particle densities is displayed in Fig. 2D. The cubes tend to align face-to-face already by assembly via simple evaporation of a dispersion droplet on a substrate [41]. More refined methods could be employed to create even denser structures, as was previously demonstrated with colloidal silica cubes [15,16].

4. Conclusions

We have established a surfactant-mediated and reproducible synthesis method for colloidal core–shell hematite@titania cubes using conventional chemicals and ambient conditions. We completed our procedure by transforming the amorphous titania shell to a porous, yet intact and uniform shell of crystalline titania to obtain non-aggregated colloidal anatase/rutile cubes. The cubes are either (partially) filled with hematite or completely hollow. These titania cubes allow for the possibility to combine the acknowledged properties of titania with the close-packing properties of cube-shaped particles.

Future research on these titania cubes could include their controlled assembly to close-packed structures and assessment of their optical and photocatalytic properties. Moreover, the titania cubes show potential as nanoreactors or nanocarriers owing to their (meso)porosity. Adsorption of CTAB onto other materials, such as amorphous silica and silver, has previously been reported [40,42,43]. Consequently, our synthesis method could be extended to core particles of different materials and shapes to create a variety of titania particles.

Acknowledgements

This research is supported by the Dutch Technology Foundation STW, Netherlands under the partnership program STW-Hyflux CEPAration Inorganic and Hybrid Membranes (project number 11020). We thank Roel Baars for his help with the graphical abstract.

Appendix A. Supplementary data

Supplementary data associated with this article can be found, in the online version, at http://dx.doi.org/10.1016/j.colsurfa.2016.05.079.

References

[1] X. Chen, S. Mao, Titanium dioxide nanomaterials: synthesis, properties, modifications, and applications, Chem. Rev. 107 (7) (2007) 2891–2959.
[2] G. Morris, W. Skinner, P. Self, R. Smart, Surface chemistry and rheological behaviour of titania pigment suspensions, Colloids Surf. A: Physicochem. Eng. Asp. 155 (1) (1999) 27–41.
[3] M. Hoffmann, S. Martin, W. Choi, D. Bahnemann, Environmental applications of semiconductor photocatalysis, Chem. Rev. 95 (1) (1995) 69–96.
[4] H. Li, Z. Bian, J. Zhu, D. Zhang, G. Li, Y. Huo, H. Li, Y. Lu, Mesoporous titania spheres with tunable chamber structure and enhanced photocatalytic activity, J. Am. Chem. Soc. 129 (27) (2007) 8406–8407.
[5] J. Joo, Q. Zhang, I. Lee, M. Dahl, F. Zaera, Y. Yin, Mesoporous anatase titania hollow nanostructures though silica-protected calcination, Adv. Funct. Mater. 22 (1) (2012) 166–174.
[6] B. O'Regan, M. Grätzel, A low-cost, high-efficiency solar cell based on dye-sensitized colloidal TiO_2 films, Nature 353 (1991) 737–740.
[7] M. Grätzel, Perspectives for dye-sensitized nanocrystalline solar cells, Prog. Photovolt.: Res. Appl. 8 (1) (2000) 171–185.
[8] S.-C. Yang, D.-J. Yang, J. Kim, J.-M. Hong, H.-G. Kim, I.-D. Kim, H. Lee, Hollow TiO_2 hemispheres obtained by colloidal templating for application in dye-sensitized solar cells, Adv. Mater. 20 (5) (2008) 1059–1064.
[9] P. Wang, D. Chen, F. Tang, Preparation of titania-coated polystyrene particles in mixed solvents by ammonia catalysis, Langmuir 22 (10) (2006) 4832–4835.
[10] M. Anderson, M. Gieselmann, Q. Xu, Titania and alumina ceramic membranes, J. Membr. Sci. 39 (3) (1988) 243–258.
[11] J. Wijnhoven, W. Vos, Preparation of photonic crystals made of air spheres in titania, Science 281 (5378) (1998) 802–804.
[12] A. Demirörs, A. Jannasch, P. van Oostrum, E. Schaeffer, A. Imhof, A. van Blaaderen, Seeded growth of titania colloids with refractive index tunability and fluorophore-free luminescence, Langmuir 27 (5) (2011) 1626–1634.
[13] Y. Jiao, F. Stillinger, S. Torquato, Optimal packings of superballs, Phys. Rev. E 79 (4) (2009) 041309.
[14] R. Ni, A.P. Gantapara, J. de Graaf, R. van Roij, M. Dijkstra, Phase diagram of colloidal hard superballs: from cubes via spheres to octahedra, Soft Matter 8 (34) (2012) 8826–8834.
[15] L. Rossi, S. Sacanna, W. Irvine, P. Chaikin, D. Pine, A. Philipse, Cubic crystals from cubic colloids, Soft Matter 7 (9) (2011) 4139–4142.
[16] J. Meijer, F. Hagemans, L. Rossi, D. Byelov, S. Castillo, A. Snigirev, I. Snigireva, A. Philipse, A. Petukhov, Self-assembly of colloidal cubes via vertical deposition, Langmuir 28 (20) (2012) 7631–7638.
[17] S. Castillo, C. Pompe, J. van Mourik, D. Verbart, D. Thies-Weesie, P. de Jongh, A. Philipse, Colloidal cubes for the enhanced degradation of organic dyes, J. Mater. Chem. A 2 (2014) 10193–10201.
[18] S. Castillo, Cubic colloids. Synthesis, functionalization and applications, (Ph.D. thesis), Universiteit Utrecht, 2015.
[19] B. Yoldas, Hydrolysis of titanium alkoxide and effects of hydrolytic polycondensation parameters, J. Mater. Sci. 21 (3) (1986) 1087–1092.
[20] W. Li, J. Yang, Z. Wu, J. Wang, B. Li, S. Feng, Y. Deng, F. Zhang, D. Zhao, A versatile kinetics-controlled coating method to construct uniform porous TiO_2 shells for multifunctional core–shell structures, J. Am. Chem. Soc. 134 (29) (2012) 11864–11867.
[21] I. Pastoriza-Santos, D. Koktysh, A. Mamedov, M. Giersig, N. Kotov, L. Liz-Marzán, One-pot synthesis of Ag@TiO_2 core–shell nanoparticles and their layer-by-layer assembly, Langmuir 16 (6) (2000) 2731–2735.
[22] K.S. Mayya, D. Gittins, F. Caruso, Gold-titania core–shell nanoparticles by polyelectrolyte complexation with a titania precursor, Chem. Mater. 13 (11) (2001) 3833–3836.
[23] A. Demirörs, A. van Blaaderen, A. Imhof, A general method to coat colloidal particles with titania, Langmuir 26 (12) (2010) 9297–9303.
[24] Y. Wang, T. Tian, X. Liu, G. Meng, Titania membrane preparation with chemical stability for very hash environments applications, J. Membr. Sci. 280 (1) (2006) 261–269.
[25] T. Sugimoto, K. Sakata, Preparation of monodisperse pseudocubic α-Fe_2O_3 particles from condensed ferric hydroxide gel, J. Colloid Interface Sci. 152 (2) (1992) 587–590.
[26] E. Barrett, L. Joyner, P. Halenda, The determination of pore volume and area distributions in porous substances. I. Computations from nitrogen isotherms, J. Am. Chem. Soc. 73 (1) (1951) 373–380.
[27] R. Spurr, H. Myers, Quantitative analysis of anatase–rutile mixtures with an X-ray diffractometer, Anal. Chem. 29 (5) (1957) 760–762.
[28] C. Wang, J. Ying, Sol–gel synthesis and hydrothermal processing of anatase and rutile titania nanocrystals, Chem. Mater. 11 (11) (1999) 3113–3120.
[29] D. Hanaor, C. Sorrell, Review of the anatase to rutile phase transformation, J. Mater. Sci. 46 (4) (2010) 855–874.
[30] A. Imhof, Preparation and characterization of titania-coated polystyrene spheres and hollow titania shells, Langmuir 17 (12) (2001) 3579–3585.
[31] J. Ying, C. Mehnert, M. Wong, Synthesis and applications of supramolecular-templated mesoporous materials, Angew. Chem. Int. Ed. 38 (1999) 56–77.
[32] S. Ding, F. Huang, X. Mou, J. Wu, X. Lue, Mesoporous hollow TiO_2 microspheres with enhanced photoluminescence prepared by a smart amino acid template, J. Mater. Chem. 21 (13) (2011) 4888–4892.
[33] H. Shibata, T. Ogura, T. Mukai, T. Ohkubo, H. Sakai, M. Abe, Direct synthesis of mesoporous titania particles having a crystalline wall, J. Am. Chem. Soc. 127 (47) (2005) 16396–16397.
[34] H. Shibata, H. Mihara, T. Mukai, T. Ogura, H. Kohno, T. Ohkubo, H. Sakai, M. Abe, Preparation and formation mechanism of mesoporous titania particles having crystalline wall, Chem. Mater. 18 (9) (2006) 2256–2260.
[35] T. Sakai, H. Yano, H. Shibata, T. Endo, K. Sakamoto, H. Fukui, N. Koshikawa, H. Sakai, M. Abe, Pore-size expansion of hexagonal-structured nanocrystalline titania/CTAB nanoskeleton using cosolvent organic molecules, Colloids Surf. A: Physicochem. Eng. Asp. 371 (1) (2010) 29–39.
[36] S. Eiden-Assmann, J. Widoniak, G. Maret, Synthesis and characterization of porous and nonporous monodisperse colloidal TiO_2 particles, Chem. Mater. 16 (2004) 6–11.

[37] C. Liu, J. Li, J. Qi, J. Wang, R. Luo, J. Shen, X. Sun, W. Han, L. Wang, Yolk-shell $Fe^0@SiO_2$ nanoparticles as nanoreactors for Fenton-like catalytic reaction, ACS Appl. Mater. Interfaces 6 (2014) 13167–13173.
[38] M. Xiao, C. Zhao, H. Chen, B. Yang, J. Wang, "Ship-in-a-bottle" growth of noble metal nanostructures, Adv. Funct. Mater. 22 (21) (2012) 4526–4532.
[39] G. de, A.A. Soler-Illia, A. Louis, C. Sanchez, Synthesis and characterization of mesostructured titania-based materials through evaporation-induced self-assembly, Chem. Mater. 14 (2) (2002) 750–759.
[40] H. Sakai, T. Kanda, H. Shibata, T. Ohkubo, M. Abe, Preparation of highly dispersed core/shell-type titania nanocapsules containing a single Ag nanoparticle, J. Am. Chem. Soc. 128 (15) (2006) 4944–4945.
[41] R. Deegan, O. Bakajin, T. Dupont, G. Huber, S. Nagel, T. Witte, Capillary flow as the cause of ring stains from dried liquid drops, Nature 389 (6653) (1997) 827–829.
[42] X. Guo, Y. Deng, D. Gu, R. Che, D. Zhao, Synthesis and microwave absorption of uniform hematite nanoparticles and their core–shell mesoporous silica nanocomposites, J. Mater. Chem. 19 (37) (2009) 6706–6712.
[43] B. Bijsterbosch, Characterization of silica surfaces by adsorption from solution. Investigations into the mechanism of adsorption of cationic surfactants, J. Colloid Interface Sci. 47 (1) (1973) 186–198.